JOURNAL OF MATERIALS SCIENCE 29 (1994) 2835–2840

Interaction between precipitating phases in quenched Al–Cu–Si alloys

M. J. STARINK*, P. VAN MOURIK
Laboratory of Metallurgy, Delft University of Technology, Rotterdamseweg 137, 2628 AL Delft, The Netherlands

The precipitation in two solution-treated Al–Cu–Si alloys, one with and one without free silicon particles, was studied by differential scanning calorimetry, X-ray diffraction and hardness measurements. In both alloys, θ′-phase and Si-phase precipitation processes proceed simultaneously. As in binary Al–Si and Al–Cu alloys aged at the same temperature, precipitation occurs at clearly separate time intervals; this finding suggests an interaction between the two precipitation processes. It is shown that the interaction of stress fields around newly formed precipitates can result in a significant decrease of the nucleation barrier and thus can explain the synchronous precipitation. The activation energy of the combined precipitation reaction is 0.95 ± 0.06 eV.

1. Introduction

The Al–1.3 at % Cu–19.1 at % Si alloy produced via melt spinning and subsequent extrusion combines the attractive properties of aluminium alloys with a large volume percentage of finely distributed silicon particles (low thermal expansion and reduced wear), giving the possibility of age-hardening of the matrix. Recently, precipitation in the solution-treated and subsequently quenched Al–1.3 at % Cu–19.1 at % Si alloy was studied by differential scanning calorimetry (DSC) [1]. It was observed that for heating rates smaller than 20 K min^{-1} the precipitation of the Si and θ′ phases from the supersaturated Al-rich phase occurs simultaneously. As in quenched binary Al–Si and Al–Cu alloys aged at the same temperature, precipitation occurs at clearly separate time intervals, this finding is somewhat surprising.

The altered precipitation kinetics in the Al–Cu–Si alloy, as compared to those in the respective binary alloys, might be due to the presence of misfitting silicon particles which influence the kinetics of precipitation from the matrix [2–6]. This influence is usually explained as follows. The difference in shrinkage on cooling, due to the difference in the respective values of coefficients of thermal expansion (CTE) of the dispersed particles and the surrounding matrix, introduces a thermal misfit between particles and matrix. This thermal misfit is accommodated by elastic and plastic deformation of the matrix [7], the latter by the creation of misfit dislocations. These dislocations can act as extra nucleation sites (enhancing precipitation) or they can annihilate excess vacancies (retarding precipitation). The elastic stresses resulting from misfit accommodation can also influence precipitation phenomena [8, 9].

To obtain a better understanding of precipitation in Al–Cu–Si alloys with and without Si particles, precipitation experiments were performed on the Al–1.3 at % Cu–19.1 at % Si alloy and on an Al–1 at % Cu–1 at % Si alloy. In the latter alloy all silicon can be dissolved in the Al-rich phase at the homogenizing temperature. The isothermal precipitation in the solid-quenched Al–1.3 at % Cu–19.1 at % Si alloy was studied by hardness measurements and by measurement of lattice parameter variations of the Al-rich phase. The precipitation in the Al–1 at % Cu–1 at % Si alloy was studied by DSC.

2. Experimental procedure

2.1. Alloy preparation

A high-purity Al–1.3 at % Cu–19.1 at % Si alloy was produced by melt spinning and subsequent extrusion. The production route of the alloy was described earlier [1]. Specimens were solution-treated for 5 min at 793 K in a vertical tube furnace and subsequently quenched in water at room temperature. After this solution treatment, the Si-particle size in the alloy studied is ~ 1–2 μm [1]. A part of the specimens was stored at room temperature awaiting further experiments; another part was stored in liquid nitrogen. It has been shown previously [10] that this difference in storing temperature does not influence the kinetics of precipitation during artificial ageing. The quenched and aged specimens will be indicated by SQ + A, followed by the ageing temperature. The ageing treatment was performed in an oil bath with temperature stability ± 1.5 K and was concluded by a direct quench into water at room temperature.

* *Present address*: Department of Engineering Materials, University of Southampton, Highfield, Southampton SO9 5NH, U.K.

0022–2461

To study the precipitation of Cu and Si atoms from the Al-rich phase in the absence of Si particles, an Al–1 at % Cu–1 at % Si alloy (nominal content) was produced from 99.999% pure Al, 99.99% pure Si and a 99.95% pure Al–50% Cu master alloy (all percentages by weight) by conventional casting. Chemical analysis showed a content of 1.07 at % Cu and 1.01 at % Si. The ingot was homogenized at 798 K for 5 days and subsequently quenched in water at room temperature. Due to the conventional casting and the long homogenizing treatment, the Al grain size of this alloy is quite large (> 0.1 mm).

2.2. X-ray diffraction

In Al–Cu–Si alloys, the lattice parameter of the Al-rich phase depends linearly on the amount of copper and silicon dissolved in it [10]. Both types of dissolved elements decrease the lattice parameter of the Al-rich phase. Hence lattice parameter measurements are a useful method for the study of precipitation.

For measurement of the lattice parameter of the Al-rich phase of the Al-1.3 at % Cu–19.1 at % Si alloy, XRD experiments were performed using a Debye–Scherrer (DbS) camera. The experimental procedures are described elsewhere [10].

2.3. Hardness measurements

Hardness measurements were performed after ageing at 423 K of two water-quenched specimens. One specimen had been naturally aged for 14 months between quenching and artificial ageing; the other was naturally aged for 24 h. Microhardness was measured on polished longitudinal sections through the axis of the extruded bar using a Leitz–Durimet Vickers hardness tester. For each hardness value at least ten indentations, evenly distributed over a line from the axis to the edge of the bar, were made (hardness did not depend on the radial distance to the centre of the bar). The indentation force was 0.981 N.

2.4. Differential scanning calorimetry

Samples of the Al–1 at % Cu–1 at % Si alloy were homogenized for 30 min at 793 K and subsequently quenched in water at room temperature. The samples were stored in a freezer at 263 K. For differential scanning calorimetry, a DuPont 910 DSC was used. Inside the DSC cell a protective gas atmosphere was maintained by flushing with 99.999% pure argon. Both specimen and reference were enclosed in an aluminium pan with an aluminium cover. Heating rates between 1 and 60 K min^{-1} were used. Per specimen, two scans were performed; the second after cooling at about 0.5 K min^{-1}. As a consequence of this low cooling rate, it can be expected that in this second run no precipitation occurs. The calibration procedures and baseline corrections have been described previously [11].

3. Results

3.1. The Al–1.3 at % Cu–19.1 at % Si alloy

Directly after quenching and after short periods of ageing, no intermetallic phases were detected by DbS experiments on the Al–1.3 at % Cu–19.1 at % Si alloy. In Table I the minimum ageing times for the appearance of the θ′ and θ phases (composition Al_2Cu) in SQ + A specimens are given. After an Al_2Cu phase had been detected, it was found to be present at all subsequent ageing times studied. The lattice parameters of the Al-rich phase as a function of ageing time are presented in Fig. 1. During ageing the Al-rich phase lattice parameter increases from values around 0.4042 nm to about 0.4051 nm. This increase is caused by the precipitation of Cu and Si atoms from the Al-rich phase (see [10]). At the final stages of ageing, the measured lattice parameter of the Al-rich phase (0.4051 nm) is higher than the value for pure Al (0.40496 nm). This is largely due to thermal stresses in the matrix caused by misfitting silicon particles [10].

TABLE I Minimum ageing times, t_m (h) required for the appearance of lines diffracted by the Al_2Cu phases in SQ + A specimens.

Phase	SQ + A 423 K	SQ + A 453 K	SQ + A 483 K
θ′	8	3.5	2
θ	512	128	16

The hardness as a function of time of artificial ageing at 423 K for two SQ Al–1.3 at % Cu–19.1 at % Si specimens is shown in Fig. 2. One specimen was naturally aged for 24 h between quenching and the start of artificial ageing, the other was naturally aged for 14 months between quenching and the start of artificial ageing. For comparison also, the lattice parameter at this temperature (from Fig. 1) and the identified phase (from Table I) are indicated in Fig. 2. The data in this figure show that (i) θ′ phase is detected from the early stages of the rise of the Al-rich phase lattice parameter, and (ii) θ phase is detected only in the final stages of the rise of the Al-rich phase lattice parameter. This observation is valid for all three ageing temperatures studied (compare Fig. 1 and Table I). This indicates that the Cu atoms precipitating from the Al-rich phase are incorporated almost exclusively in the θ′ phase.

3.2. The Al–1 at % Cu–1 at % Si alloy

The DSC run of the quenched Al–1 at % Cu–1 at % Si alloy at a heating rate of 5 K min^{-1} is presented in Fig. 3. In this run only one exothermic effect is observed between 520 and 640 K. The endothermic effect situated beyond 640 K reveals three sub-effects. The end temperatures of these three effects are about 680, 730 and 790 K. These temperatures correspond with the semi-equilibrium solvus of θ′ and the equilibrium solvi of θ and Si phase, respectively [12, 13]. These three phases are the only ones reported to exist above 600 K [1, 14]. Correspondingly, the three sub-effects are interpreted to be due to the dissolution of these three phases [1]. From this identification of the dissolution effects it is derived that the precipitation effect contains the formation of Si and θ′ phases. This formation might at least partly occur during the precipitation effect. However, the formation of θ phase might also occur during dissolution of the θ′ phase.

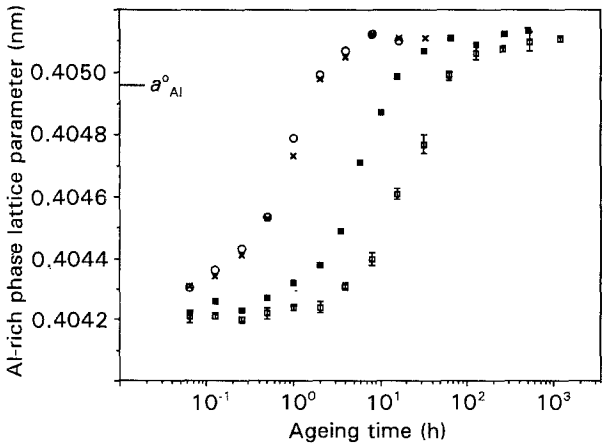

Figure 1 The Al-rich phase lattice parameters of the Al–1.3 at % Cu–19.1 at % Si alloy as a function of time of ageing at the indicated temperatures; storage between quenching and ageing was at room temperature (RT) or in liquid nitrogen (LN). The lattice parameter for pure aluminium, a^{0}_{Al}, is indicated. □, 423 K, RT; ■, 453 K, LN; ○, 483 K, RT; ×, 483 K, LN.

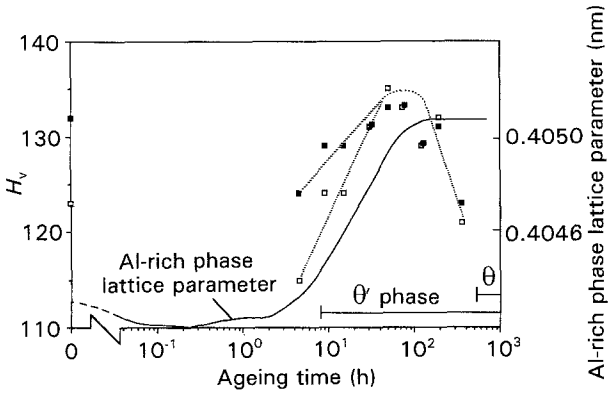

Figure 2 Hardness of two solid-quenched Al–1.3 at % Cu–19.1 at % Si specimens during ageing at 423 K. The two specimens were naturally aged for 24 h or for 14 months between quenching and artificial ageing. For comparison the Al-rich phase lattice parameter of the SQ + A423 specimen is also given (see Fig. 1). The time intervals at which the θ′ phase and the θ phase are detected are indicated. □, SQ + 24 h NA; ■, SQ + 14 months NA.

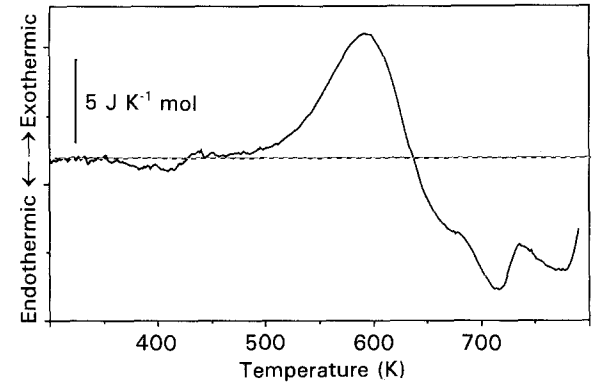

Figure 3 DSC run at 5 K min^{-1} of the SQ Al–1 at % Cu – 1 at % Si alloy.

At a heating rate of 1 K min^{-1}, similar effects were observed.

At heating rates larger than 10 K min^{-1}, the endothermic dissolution effect reveals only two sub-effects. The temperatures of these two effects indicate that they correspond to Si and θ-phase dissolution. Hence it is thought that at these heating rates only negligible amounts of θ′ phase are formed during the precipitation effect. In accordance with this, it was found that at these heating rates the precipitation effect reveals two sub-effects.

4 Discussion

4.1. Age hardening

Misfit after quenching (due to the difference in CTE of matrix and Si particles) will result in the creation of dislocations [7, 10]. These dislocations will increase the hardness of the matrix [7]. Artificial ageing generally decreases the dislocation density. Hence the observed drop in hardness of SQ Al–1.3 at % Cu–19.1 at % Si specimens after a short time of artificial ageing (see Fig. 2) is ascribed to this annealing-out of dislocations. Fig. 2 further shows that during the precipitation of copper and silicon atoms from the Al-rich phase, the hardness of the alloy increases. The increase in hardness coincides with the detection of the semi-coherent θ′ phase. As the precipitation of silicon is generally thought not to cause a hardness increase [14], it is concluded that the formation of θ′ precipitates is the main hardening mechanism in the Al–1.3 at % Cu–19.1 at % Si alloy. The hardness of the Al–1.3 at % Cu–19.1 at % Si specimen naturally aged for 14 months after solid quenching is about 10 H_V higher than that of the solid-quenched specimen. This is thought to be due to GP zones which, in this alloy, form on natural ageing for several months [1], and which increase the hardness. On artificial ageing, the difference in hardness between the two specimens gradually decreases. This might indicate that GP zones gradually dissolve. (In DSC experiments on Al–1.3 at % Cu–19.1 at % Si alloys aged at room temperature, the GP zones start to dissolve from 360 K onwards (see [1]).) Both specimens reach essentially the same maximum hardness (135 H_V) after about 60 h of ageing.

4.2. Kinetics of Si and θ′ phase precipitation

As noted above, the increase of the Al-rich-phase lattice parameter on ageing of the SQ Al–1.3 at % Cu–19.1 at % Si alloy (see Fig. 1) is due to the precipitation of Cu and Si atoms from the Al-rich phase. The curves representing the variation of the lattice parameter as functions of the ageing time (Fig. 1) are very smooth and do not show any plateau or multiple inflection points. This indicates that the precipitation of Si phase and θ′ phase strongly overlaps. This finding corresponds to DSC experiments performed on the same alloy, which show that the precipitation of Si phase and θ′ phase gives rise to a single heat-evolution effect [1]. In the present study, the DSC experiments on the Al–1 at % Cu–1 at % Si alloy, have shown that also for this alloy Si phase and θ′ phase precipitation overlap strongly (see Section 3.2 and Fig. 3). In contrast to these findings, the precipitation of alloying elements from the Al-rich phase in solid-quenched binary Al–Si and Al–Cu alloys occurs at clearly separated time intervals. In SQ Al–Si alloys the precipitation of Si occurs between about 0.01 and 0.2 h at

492 K [15]. On ageing an SQ alloy with about the same percentage of Cu atoms dissolved in the Al-rich phase (Al–1.7 at % Cu) as in the Al–1.3 at % Cu–19.1 at % Si alloy and at the same ageing temperature, the precipitation of the θ′ phase starts after about 0.5 h, and is completed in about 10 h [16]. From Fig. 1 it is obtained that in the Al–1.3 at % Cu–19.1 at % Si alloy at a similar temperature, precipitation occurs between about 0.1 and 2 h. This is intermediate between the ageing times required for precipitation in the respective binary systems. The above points at some interaction between the precipitation of Si phase and the θ′ phase.

Due to the strong overlap between the Si- and θ′-phase precipitation processes it is not possible to obtain the extent of the two precipitation processes separately. However, as the interaction between the two processes is thought to be very strong (see previous section), it is considered that the two processes are governed by one effective activation energy. To obtain this activation energy the complement of the extent of the combined reaction is defined by

$$1 - x(t) = [a_{Al}(t) - a_{Al}(t = \infty)]/[a_{Al}(t = 0) - a_{Al}(t = \infty)] \quad (1)$$

in which $a_{Al}(t)$ is the Al-rich phase lattice parameter during ageing, $a_{Al}(t = \infty)$ is the Al-rich phase lattice parameter after completion of precipitation, and $a_{Al}(t = 0)$ is the Al-rich phase lattice parameter before the start of precipitation. Arrhenius plots were constructed for $x = 0.1$, 0.2, 0.3, 0.4, 0.5, 0.6, 0.7 and 0.8. The correlation coefficients of the straight lines through these plots are all satisfactorily close to unity (all correlation coefficients are between 0.97 and 0.99). The average value of the apparent activation energy for the combined process is 0.95 ± 0.06 eV. In accordance with the assumption that one single activation energy governs the combined precipitation process (see above), no significant variations with the extent of the reaction (i.e. with x) were observed. The activation energy agrees well with the apparent activation energy of the combined Si and θ′ precipitation as obtained from DSC experiments on the same alloy (1.00 eV, see [1]). The apparent effective activation energy for precipitation in the Al–1.3 at % Cu–19.1 at % Si alloy is intermediate between the apparent activation energy of Si precipitation in solid-quenched Al–Si alloys (0.89 eV, see [17]) and the apparent activation energy of θ′ formation in solid-quenched Al–Cu (about 1.1 eV for $T < 550$ K, see [16]). This finding is consistent with the notion that the Si-phase and the θ′-phase precipitation processes interact.

4.3. Interaction between Si and θ′ phase precipitation

By TEM experiments on Al-based metal matrix composites (MMCs), it was recently shown that θ′ precipitation is very sensitive to stress fields around misfitting particles [9]. In this research it was shown that both density and preferred orientation of the plate-shaped θ′-phase precipitates are influenced by the strain fields in the matrix around a misfitting SiC particle. (In unstrained Al–Cu the orientations of the θ′-phase precipitates are equally distributed over the three possible orientations on the {1 0 0} planes of the Al-rich phase [18].) In the Al–1.3 at % Cu–19.1 at % Si alloy 21 vol % of free silicon particles are present, while in the Al–1 at % Cu–1 at % Si alloy all silicon is dissolved during homogenizing. As in both alloys the precipitation of the Si phase and the θ′ phase occurs simultaneously, it is not possible that the strain fields around free silicon particles in the Al–1.3 at % Cu–19.1 at % Si alloy are the cause for the interaction. Instead it is thought that the interaction of stress fields around newly formed precipitates is the cause of the interaction.

As the volume occupied by a silicon atom in the Si-rich phase is larger than the volume occupied by the same atom dissolved in the Al-rich phase (see [19]), the precipitation of silicon atoms from the Al-rich phase will result in misfit stresses. The formation of θ′-phase precipitates causes misfit stresses in the direction normal to the θ′ plate [20]. It has been shown by Perovic *et al.* [21, 22] that, through minimizing the interaction term of the strain fields, the formation of new θ′-phase precipitates is facilitated by the elastic strain fields of existing θ′-phase precipitates. In binary Al–Cu alloys this gives rise to the precipitation of linear arrays of θ′-phase precipitates [21, 22]. The strain fields around Si particles and those around θ′ precipitates can also interact to facilitate the formation of either of these phases. This is illustrated in Fig. 4, in which two orientations of a plate-shaped θ′ precipitate relative to a spherical Si precipitate are depicted. Since θ′ is semicoherent, the misfit of the θ′-phase plate normal to the plate is much larger than the misfit parallel to the plate. As in the nucleation stage the precipitates are too small to induce plastic

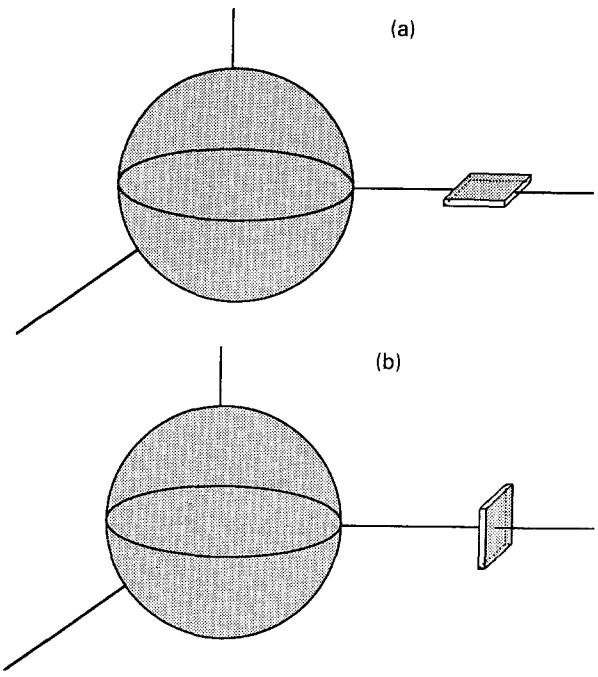

Figure 4 Two possible orientations of a plate shaped particle relative to a spherical particle: (a) the surface-normal orientation, (b) the surface-parallel orientation.

accommodation of misfit, see [23], and as thermally activated relaxation is assumed to occur only in the latter stages of precipitation, only elastic accommodation of misfit is considered. Then the 'surface-normal' orientation (Fig. 4a) is energetically favourable in the case that the sign of the misfit is equal for both precipitates. The 'surface-parallel' orientation (Fig. 4b) is energetically favourable in the case where the misfits are of opposite sign (see also [9]).

An estimation of the magnitude of this strain interaction can be obtained from the density of the strain energy in the matrix around a spherical misfitting inclusion, per unit of volume, E_{el} (see [24])

$$E_{el} = 6\mu_A C^2 \varepsilon^2 \left[\frac{r_0}{r}\right]^6 \quad (2)$$

where μ_A is the shear modulus of the matrix (i.e. of aluminium), C is a constant depending on the elastic constants of matrix and inclusion ($C = 0.73$ for Si in Al, see [23]), ε is the misfit parameter (0.0643 for Si in Al, see [18]), r_0 is the radius of the inclusion and r is the distance to the centre of the inclusion. If the formation of Cu precipitates would completely annihilate the strain energy in the matrix, then the energy available per Cu atom, E_{Cu}, amounts to

$$E_{Cu} = \frac{E_{el}}{x_{Cu}\rho_N} \quad (3)$$

where x_{Cu} is the atomic fraction of copper in the matrix (0.016 in the Al–1.3 at % Cu–19.1 at % Si alloy) and ρ_N is the atomic density of the matrix. Using values from the literature [25] the following equation is obtained (the temperature dependence of elastic constants for the small temperature range considered is neglected):

$$E_{Cu} = 2.3\,\text{eV}\left[\frac{r_0}{r}\right]^6 \quad (4)$$

In a similar manner, an estimate of the average energy available to one copper atom (which depends linearly on the volume fraction of newly formed Si precipitates) is obtained (see [24]):

$$\overline{E_{Cu}} = 0.023\,\text{eV} \quad (5)$$

From Equation 4 it can be concluded that for a significant part of the matrix (i.e. $r < 2r_0$), the energy available to one copper atom is sufficiently large to explain the observed decrease of the activation energy for precipitation in the Al–Cu–Si alloy ($E_A = 0.95$ eV) as compared to that in binary Al–Cu alloys ($E_A = 1.1$ eV). The average energy available to one copper atom (0.023 eV, Equation 5) seems a little too low to explain this difference. However, it should be noted that θ′-phase precipitates will preferentially nucleate on sites where the barrier for nucleation is lowest, i.e. where the elastic energy density is highest. Hence this value should be considered to be an estimated lower limit for the energy available.

Experimental indications for the importance of misfit strains on the precipitation of θ′ phase can be obtained from the work of Hosford & Agrawal [18], who showed that a uniaxial stress of 48 MPa has a profound influence on θ′-phase precipitation in quenched Al–1.7 at % Cu alloys: under compression along a ⟨1 0 0⟩ direction the precipitation on {1 0 0} planes parallel to the stress axis is favoured, while in tension precipitation on {1 0 0} planes perpendicular to the stress axis is favoured. For stresses of 34.5 MPa and lower, no difference in density of θ′-phase precipitates on the three {1 0 0} planes was observed. These externally applied uniaxial stresses can be compared with the stresses around misfitting inclusions. The stress distribution in the matrix around a spherical misfitting inclusion is given by (in spherical coordinates) [24]:

$$\sigma_r = -2\sigma_\theta = -4\mu_A C\varepsilon\left(\frac{r_0}{r}\right)^3 \quad (6)$$

For Si precipitates in Al, the following equation is found:

$$\sigma_r = -2\sigma_\theta = -5.1\,\text{GPa}\left(\frac{r_0}{r}\right)^3 \quad (7)$$

This shows that for $r < 5r_0$ θ′-phase precipitation will be influenced by misfit stresses. Hence after completed precipitation of silicon (corresponding to about 1 vol % of newly formed Si particles), the whole of the matrix will be affected.

The above shows that strain fields around Si precipitates influence θ′-phase formation by lowering nucleation barriers. This may explain why the precipitation of the θ′ and Si phases from the Al-rich phase in the Al–Cu–Si alloy proceeds synchronously.

5. Conclusions

During ageing of quenched Al–Cu–Si alloys, the θ′-phase and Si-phase precipitation processes occur simultaneously. This can be explained by interaction of stress fields around newly formed precipitates. The activation energy of the combined precipitation reaction is 0.95 ± 0.06 eV.

Acknowledgements

The authors are indebted to Mr P. de Ruiter and Mr H. Kleinjan for providing the melt-spun and conventionally cast alloys, to Dr J. Duszczyk and Dr Zhou Jie for performing the extrusion, to Ing. N. M. van der Pers and Mr J. F. van Lent for assistance with the XRD experiments, to students M. van der Meerakker, P. de Haan, K. M. Mussert and N. Schipper for performing the DSC experiments, and to Ing. N. Geerlofs for assistance with the DSC experiments. The financial support of the Foundation for Fundamental Research of Matter and for Technological Sciences (FOM/STW) is gratefully acknowledged.

References

1. M. J. STARINK and P. VAN MOURIK, *Metall. Trans.* **22A** (1991) 665.
2. T. CHRISTMAN and S. SURESH, *Acta Metall.* **36** (1988) 1691.
3. J. M. PAPAZIAN, *Metall. Trans.* **19A** (1988) 2945.
4. T. S. KIM, T. H. KIM, K. H. OH and H. I. LEE, *J. Mater. Sci.* **27** (1992) 2599.

5. I. DUTTA, S. M. ALLEN and J. F. HAFLEY, *Metall. Trans.* **22A** (1991) 2553.
6. M. J. STARINK, V. JOORIS and P. VAN MOURIK, in Proceedings of the 12th Risø International Symposium on Metal Matrix Composites – Processing, Microstructure and Properties, Roskilde, Denmark, September 2–6, 1991, edited by N. Hansen, D. J. Jensen, T. Leffers, H. Lilholt, T. Lorentzen, A. S. Pedersen, O. B. Pedersen and B. Ralph (RISO National Laboratory, Roskilde, Denmark, 1991) p. 675.
7. M. TAYA, K. E. LULAY and D. J. LLOYD, *Acta Metall. Mater.* **39** (1991) 73.
8. M. J. STARINK and P. VAN MOURIK, in Proceedings of the International Conference on Advanced Al and Mg Alloys, Amsterdam, The Netherlands, June 20–22, 1990, edited by T. Khan and G. Effenberg (ASM International, Brussels, 1991) p. 695.
9. P. B. PRANGNELL and W. M. STOBBS, in Proceedings of the 12th Risø International Symposium on Metal Matrix Composites – Processing, Microstructure and Properties, Roskilde, Denmark, September 2–6, 1991, edited by N. Hansen, D. J. Jensen, T. Leffers, H. Lilholt, T. Lorentzen, A. S. Pedersen, O. B. Pedersen and B. Ralph (RISO National Laboratory, Roskilde, Denmark, 1991) p. 603.
10. M. J. STARINK, P. VAN MOURIK and B. M. KOREVAAR, *Metall. Trans. A*, **24A** (1993) 1723.
11. M. J. STARINK, V. JOORIS and P. VAN MOURIK, in Proceedings of the 12th Risø International Symposium on Metal Matrix Composites – Processing, Microstructure and Properties, Roskilde, Denmark, September 2–6, 1991, edited by N. Hansen, D. J. Jensen, T. Leffers, H. Lilholt, T. Lorentzen, A. S. Pedersen, O. B. Pedersen and B. Ralph (RISO National Laboratory, Roskilde, Denmark, 1991) p. 675.
12. J. L. MURRAY, *Int. Metall. Rev.* **30** (1985) 211.
13. H. W. L. PHILLIPS, "Annotated Equilibrium Diagrams of Some Aluminium Alloy Systems", Institute of Metals Monograph and Report Series No. 25 (Institute of Metals, London, 1959) p. 15.
14. L. F. MONDOLFO, "Aluminum Alloys: Structure and Properties" (Butterworths, London, 1976) p. 372.
15. P. VAN MOURIK, E. J. MITTEMEIJER and TH. H. DE KEIJSER, *J. Mater. Sci.* **18** (1983) 2706.
16. P. MERLE, F. FOUQUET and J. MERLIN, *Scripta Metall.* **15** (1981) 373.
17. M. VAN ROOYEN and E. J. MITTEMEIJER, *Metall. Trans.* **20A** (1989) 1207.
18. W. H. HOSFORD and S. P. AGRAWAL, *ibid.* **6A** (1975) 487.
19. E. J. MITTEMEIJER, P. VAN MOURIK and TH. H. DE KEIJSER, *Phil. Mag. A* **43** (1981) 1157.
20. W. M. STOBBS and G. R. PURDY, *Acta Metall.* **26** (1978) 1069.
21. V. PEROVIC, G. R. PURDY and L. M. BROWN, *ibid.* **27** (1979) 1075.
22. *Idem, ibid.* **29** (1981) 889.
23. J. K. LEE, Y. Y. EARMME, H. I. AARONSON and K. C. RUSSELL, *Metall. Trans.* **11A** (1980) 1837.
24. P. VAN MOURIK, TH. H. DE KEIJSER, N. M. VAN DER PERS and E. J. MITTEMEIJER, *Scripta Metall.* **22** (1988) 1547.
25. C. J. SMITHELLS (ed.), "Metals Reference Book", 5th ed (Butterworths, London, 1976) p. 975.

Received 23 August
and accepted 10 November 1993